FTM2001-07; August 31, 2001,Version 1.2

A Proposal For Additional Photometric Bands, II

3D Classification without a u' band

Rob Olling

USNO/USRA, Washington, DC

ABSTRACT

This memo is a sequel to the photometric memo (FTM2001-03). I tabulate the current version of the proposed 6+1 filter set. In addition, I present classification results for possible filter sets that do not include a u' band. Such filter sets behave somewhat worse. At V=15, I find: for $T_{eff}, A_V, R_V, log(g)$ and $[Fe/H]$ I find errors of: 3.7%, 60 mmag, 1.0% 0.4 dex and 0.8 dex for a 6+1 NO-u' band system. The corresponding values for the 7+1 YES-u' band filter set as reported in FTM2001-03 are: 3%, 50 mmag, 1.1%, 0.4 dex and 0.6 dex, respectively.

In addition to these result, I present results that are approximately the theoretically best possible classification values. As compared to YES-u' sets, NO-u' filter sets perform slightly better between 6,000K and 10,000K, and about twice worse above 11,000K.

I also show that transformation between photometric systems (e.g., SDSS and UVBRI) depend strongly upon metallicity and surface gravity. Thus, color transformations only make sense for groups of stars with identical physical parameters.

1. Introduction

In a previous memo (FTM2001-03) a proposal was presented to use eight photometric bands for the FAME mission so as to be able to perform 3+2-dimensional stellar classification. The physical basis for 5D classification employing intermediate-band photometry is the fact that the effects of temperature, surface gravity and metallicity manifest themselves not only by changes in the detailed line-shapes, but also the shape and amplitude of the spectrum on scales of tens of nanometers. With an 6+1 band filter set, the three stellar astrophysical parameters as well as the two interstellar extinction parameters can be determined rather well. To first order, the classification accuracy is proportional to the signal-to-noise ratio

Table 1: Properties of the recommended filter system **with** a u' filter. The band designations, central wavelengths FWHM and system throughput are listed in the first 4 columns. The 5^{th} gives the estimated single-observation accuracies (δm_S). The mission-end precision is tabulated in #6. These numbers include the actual throughput (#4) and CCD covering fraction (#7). The mission-end number of observations is listed in #8. The bracketed TiO_C filter is used for bright-star astrometry. The average δm_M equals 9.6 mmag. On average, this 7-band system has errors 76% worse than the 4-band SDSS system. Note the changes in central wavelength and bandwidth for F411 with respect to FTM2001-03.

filter name (1)	λ_0 [nm] (2)	$FWHM$ [nm] (3)	$< TP >$ (4)	δm_S [mmag] (5)	δm_M [mmag] (6)	F_{CCD} (7)	N_{obs} (8)
u'	352	63	0.14	145	16.0	1.14	81.6
F411	411	50	0.56	83	10.6	0.84	60.4
g'	480	141	0.76	42	7.9	0.40	28.6
r'	625	139	0.83	41	7.6	0.40	28.6
(TiO_C	745	30	0.73	93	6.4	3.00	214.3)
i'	769	154	0.68	43	7.9	0.40	28.6
PaJ/Ca II	875	85	0.45	71	10.6	0.62	44.4

per filter (cf. figure 8 of FTM2001-03). The SDSS u' filter is part of the FTM2001-03 filter set. However, it may be that a u' filter can not be calibrated on-board or has too low overall throughput. In that case absolute and even relative photometry becomes very difficult. In this memo I present some results for filter sets that do not include a u' band, or have significantly reduced u' band throughput. The classification disadvantage incurred by not having u' data is in part compensated by the fact that the other filters will have a larger CCD area assigned, and hence more transits, and hence better final signal-to-noise ratio per band.

Several non-u' filter sets mutations of the blue part of the bandpass are possible. The program that I use to perform 5D classification in FTM2001-03 only barely distinguishes between those variants. Color-color plots and a new classification scheme described below indicate that the best results are obtained for a system that has largest overlap with the Strömgren/Vilnius systems: that is to say, without the SDSS g' band[1]. However, there is a filter set that *does* include the g' band which performs only slightly worse than the best possible non-u' non-g' combination. The properties of this filter set are tabulated in table 2.

[1]This set consists of the following band/FWHM combination: 411/50, 466/50, 520/50, 625/139, 745/30, 769/154, 875/85, where 520, 625 and 769 correspond to the Mg b, r' and i' bands.

Table 2: Properties of a good filter system **without** a u' filter. For column identifications, see table 1. The average mission-end photometric accuracy equals 8.4 mmag.

filter name (1)	λ_0 [nm] (2)	$FWHM$ [nm] (3)	$< TP >$ (4)	δm_S [mmag] (5)	δm_M [mmag] (6)	F_{CCD} (7)	N_{obs} (8)
F411	411	50	0.56	83	9.1	1.14	81.6
F466	466	50	0.76	71	9.8	0.73	52.3
g'	480	141	0.76	42	7.9	0.40	28.6
r'	625	139	0.83	41	7.6	0.40	28.6
(TiO_C	745	30	0.73	93	6.4	3.00	214.3)
i'	769	154	0.68	43	7.9	0.40	28.6
PaJ/Ca II	875	85	0.45	71	9.8	0.73	52.4

Applying the flux-and-color χ^2 minimization classification scheme outlined in FTM2001-03, NO-u' filter sets perform a bit worse than YES-u' sets. Some results are graphically presented in figure 2. At V=15, and for $T_{eff}, A_V, R_V, log(g)$ and $[Fe/H]$ I find errors of: 3.7%, 60 mmag, 1.0% 0.4 dex and 0.8 dex for a 6+1 NO-u' band system. The corresponding values for the 7+1 YES-u' band filter set as reported in FTM2001-03 are: 3%, 50 mmag, 1.1%, 0.4 dex and 0.6 dex, respectively.

2. Filter Set Properties

Below I enumerate some of the useful properties of possible FAME bands. Note that I have somewhat changed the central wavelengths and/or bandwidths of the blue intermediate bands with respect to FTM2001-03.

- **u':** In combination with g' (or r'), this band characterize the Balmer jump, a gravity indicator for hotish stars ($T_{eff} \gtrsim 5,000$ K). The line-blanketing effect is also well constrained by u', so that this band has excellent $[Fe/H]$ sensitivity for all but the hottest stars.

- **F411:** This band is centered close to the Strömgren v and the Vilnius X bands. In combination with g' (or r'), this bands characterize the line-blanketing effects due to metallicity. The $[Fe/H]$ sensitivity of F411 is about half as strong as that of u'. Some surface gravity sensitivity occurs for $9,000K \lesssim T_{eff} \lesssim 6,500K$ and below 4,500K.

- **F466:** This band is centered close to the central wavelength of the Strömgren b and the Vilnius Y bands, and is an alternative for the g' band. The SDSS g' contains

significant part of the line-blanketing of the F411 band, and the whole Mg b complex. As such, g' is not a "clean" measure of either spectral property.

- **Mg b @ 520 nm:** This line is a well-known (DDO52, Vilnius Z) surface gravity indicator for **cool** stars. Over the whole temperature range, metallicity is a more important factor (cf., bottom panels of fig. 4). Also, the gravity effect diminishes significantly towards lower metallicities (cf., top panels of fig. 4).
- **PaJ/Ca II triplet @ 875 nm:** This band is primarily a gravity indicator for hot stars (cf. fig. 5). This band lies just red-wards of the Pachen jump, and contains the NIR Ca II triplet. Metallicity only affects this band below $T_{eff} \sim 5,500K$, and low gravities. Contrary to the Mg b complex, the Ca II signature increase in strength with decreasing surface gravity. This band is a very good gravity indicator for stars in the instability strip ($5,500K \lesssim T_{eff} \lesssim 8,500K$, $0.0 \lesssim r' - i' \lesssim 0.3$, cf. fig. 5), albeit that the S/N is rather low.
- **TiO-continuum band @ 745 nm:** This 30 nm wide band sits right between two very deep TiO absorption bands in late-type stars. A TiO index can be constructed from r' and TiO_C. This index would measure that measures metallicity in late-K and M-type stars. It would also serve as a valuable diagnostic to distinguish between reddened blue stars and low-extinction red stars. Since hot stars have no features in this band either, the TiO_C band is an ideal continuum band.

Note that all filters (Mg b/g', TiO & PaJ/Ca II) centered on prominent "metal" lines actually measure the α-elements abundance, *not the iron abundance*. Because iron lines are prevalent in stellar spectra, all bands are sensitive to the overall metallicity. However, the F411 is specifically chosen to measure the region where overall metallicity has its strongest signature: the region of significant line-blanketing region, just red-wards of the Balmer jump.

There have been some iterations before the filters in table 1 were chosen. The conclusion is that the two blue bands significantly improve the performance of the classification scheme. Also, classification results improve when the central wavelengths and widths are chosen to be similar to their Strömgren/Vilnius equivalents. I have not investigated any filter sets with bands narrower than 50 nm.

In figures 3 through 5, I present some color-color diagrams that illustrate the "resolution" that can be obtained in 3D classification. In each panel, color-color diagrams are shown with one parameter fixed. Each line corresponds to a temperature sequence. The effects of varying metallicity at constant $log(g)$ are shown in the bottom panels. The top panels show the effects of gravity at constant $[Fe/H]$. Typically, the classification resolution is less in other color-color plots.

3. Classification Resolution

The label that is present in the bottom-left corner of each panel reports the maximum color separation between the models plotted at a given temperature. For example, in the lower-right panel of fig. 3, the separation between the $[Fe/H] = -3$ and $[Fe/H] = 0$ models at $T_{eff} = 4,500$K equals 681 mmag. Given the throughout and number of observations tabulated in table 1, a star of this effective temperature will have a mission-end photometric accuracy of $\delta(F411 - F625) = 19.6$ mmag. That is to say, the models of extreme metallicity are separated by 34.8 photometric standard deviations ($N_\sigma = 34.8$). I define the "classification resolution" to be the range in the classification parameter divided by the number of σ that separate those models. In the above example, $F411 - F625$ has a metallicity resolution of $\rho = \delta[Fe/H]/N_\sigma = 0.09$ dex at $T_{eff} = 4,500$K and $log(g) = 4.5$. Inspection of these figures indicates that the classification resolution depends on all three stellar parameters.

3.1. The Best Possible Classification?

As explained in FTM2001-03, the best classification is obtained by selectively combining information from different color-color combinations. Below I present an attempt to achieve optimal classification results. For this case I do not consider the effects of interstellar extinction, so that the results will be over-estimates of the classification possibilities attainable by FAME.

The process is based on a slight alteration of the concept of classification resolution. I determine the resolution for each parameter X_i for each color i from the temperature-color data directly[2]. If we assume that the error on X_i equals the classification resolution, the true value of parameter X equals the weighted sum on the determinations in all colors: $\overline{X} = \sum_i w_i X_i$, where $w_i = 1/\rho_i^2$. The final classification resolution, or equivalently, the error on $\overline{X}$ is given by:

$$\delta X \sim 1.0/\sqrt{\sum_{i=0}^{i=N_C} \frac{1}{\rho_i^2(X)}} \quad (1)$$

In practice, it is best to only include those N_C bands that have the best ρ_i values: below I use $N_C = 7$. Fewer colors degrade the classification resolution[3], more colors hardly improve the results. This procedure is an approximation to reality in the sense that it assumes that

[2]At some constant value of the other parameter.

[3]For $N_C = 1$, the results are about twice worse.

the models are equally spaced[4] in parameter X.

The metallicity classification errors will depend on T_{eff} and $log(g)$, while gravity classification varies with T_{eff} and $[Fe/H]$. I present best possible classification errors in figures 6 and 7. Analogous to the previously presented figures, the top and bottom panels report the surface gravity and metallicity classification resolution results (at fixed metallicity and gravity, respectively). Several inferences can be made from these figures:

1. 3D classification can be done rather well
2. Classification results most strongly depend on effective temperature
3. Surface gravity classification is most difficult for G-type stars with $T_{eff} = 5,000 \pm 500K$
4. Metallicity determination is poor for A-type stars with $8,000 \lesssim T_{eff} \lesssim 10,000$K
5. Surface gravity determination is hardly affected by poorly known metallicities for A-type stars.
6. Gravity and metallicity classification is excellent below $T_{eff} = 4,500$K, i.e. for K giants and dwarfs
7. u' band photometry has its largest impact for temperatures larger than 10,000 K (cf. figures 6 and 7).
8. In the $T_{eff} \gtrsim 10,000$ K range, $log(g)$ and $[Fe/H]$ resolution are about twice worse without u' band.
9. A factor two change in the throughput of the u' band will change the gravity resolution for G-type stars by 0.1 dex (more photons is better).

The difficulty determining metallicity for A-type stars is well known: due to the enhanced H^- continuum opacity, the line-to-continuum opacity ratio is small, so that the metal lines become weak, so that metallicity has only a small effect on the stellar spectra. The shift of low-$[Fe/H]$ resolution peak towards higher temperatures for larger $log(g)$ is considerable, and due to the fact that the onset of the H^- opacity shifts towards higher temperatures at higher pressure ($log(g)$.

[4]The classification resolution ρ can be slightly re-formulated: $\rho = \Delta X/(\Delta C/E_C)$, with ΔX the range in parameter X, C the color i and E_C the error on color i. In this case we arrive at a more accurate definition of the classification resolution: $\rho_i(C) = E_C(C) \times \frac{\delta X}{\delta C}$, where the gradient is evaluated at C.

At this point, I do not understand the gravity problem for G-type stars.

A reduction of the width of the bandpasses of the F411 and F466 bands to 50 nm results in ~ 0.2 dex better gravity resolution for solar metallicity G stars. For stars earlier than A, the narrow F411 and F466 filters results in slightly worse (0.05 dex) gravity classification.

For cool stars, the g' band basically measures the Mg b line. It is thus expected that better results can be obtained with a narrower Mg b filter: that is to say, replace g' by the Mg b/F516 filter. In practice, the NO-g' classification results are only marginally better than the YES-g' results.

The classification resolution "bumps" evident in figures 6 and 7 were not noticed in FTM2001-03. This is due to the fact that the temperature bins employed in FTM2001-03 were rather large.

4. Practical Filter-CCD Combinations

In the 6+1 filter set layout, 6 photometric filters are spread out over 4 CCDs. The seventh filter resides on the bright-star CCDs. For redundancy purposes, each of the photometric filters needs to be present on two different CCDs. Furthermore, so as to avoid inter-filter gaps as much as possible, we would accommodate three filters per CCD. Furthermore, so as to optimize throughput/QE, we would want to group "blue" and "red" filters on different chips. However, the CCD area assigned to the three bluest and reddest bands do not allow for such as scheme. From table 1 we find[5] $A_{3,blue} = 2.38$ and $A_{3,red} = 1.42$, whereas there should be 1.9 CCD per color group.

One way to approximately solve this problem is to have the blue group consist of u' and F411 only, and have all other filters in the other group. That would yield areas: $A_{2,blue} = 1.98$ and $A_{4,red} = 1.82$, tolerably close to the 1.9 CCD/group requirement. Alternatively, we could combine the bluest and reddest bands onto one group. In that case we would have: $A_{outer} = 1.76$ and $A_{inner} = 2.04$. However, both scenarios would require 4 filters and three inter-filter gaps on one of the CCD groups. The first scenario would be preferable since it would allow for optimization of the CCD's anti-reflection coating, and hence the total throughout.

Can we change the tabulated CCD fractions? The allocation of CCD area per band was achieved by combining two conflicting requirements: 1) to achieve equal mission-end photometric accuracy per band and 2) make sure that a minimum amount of transits occurs per filter. In order to ensure at least 28 transits per filter, I assign a minimum area of 0.4

[5]The total is 5% smaller than 4 due to the unavoidable inter-filter gaps.

CCDs per filter: this minimum should not be lowered. It would be possible but tricky to add another constraint on the sum of the CCD area per 3-consecutive filter group. The major effect would be to reduce the silicon area for the three bluest bands by 0.48 CCD, while the three reddest bands would gain that much.

4.1. Shuffling Silicon Real Estate

It is obvious that such a big reallocation of CCD area could significantly change the classification resolution. This task requires some guidance by the classification experience acquired to-date.

The rather poor u' mission-end sensitivity suggests that u' real estate should not be compromised. However the classification features probed by u' (the Balmer jump for hot stars and line-blanketing for F&G-type stars) is quite strong in stars that have significant u' flux[6]. In fact, the results from my experiments in §§3.1, point 9 show that changing the number of u' transits by a factor of two hardly affects the classification results. Thus, a certain classification resolution can be achieved by relatively poor u' photometry, while much better data is required employing weaker features. For example, the PaJ/Ca II feature is a good surface gravity indicator for stars in the blue part of the instability strip, but its utility is very much S/N limited (cf. figure 5).

I have experimented with a scheme where the 3-blue and 3-red groupings are retained, while I decreased the u' area substantially and increased the PaJ/Ca II covering fraction[7]. The classification resolution is only slightly affected. Worse u' & better PaJ/Ca II data leads to: 0.05 dex worse $log(g)$ results for G-type stars, 0.1 dex better $[Fe/H]$ for $8,000 \lesssim T_{eff} \lesssim 10,000$ K, and 0.05 dex worse $[Fe/H]$ for O/B stars.

5. Color Transformations

Depending on surface gravity and metallicity, stars of a given T_{eff} will have different fluxes in a given band. This is the principle that underlies 3D spectral classification with intermediate-band photometry. As a result, transformations between one photometric system and another system become $log(g)$ and $[Fe/H]$ dependent. I illustrate this effect in figure 8. Each curve corresponds to a temperature sequence at a given gravity and metallicity (after a reference linear relation has been subtracted from all curves). Most curves differ

[6]Obviously, that is the very reason that "UV" bands have played such a prominent role in the the classification of stars.

[7]F_{CCD} = 0.8, 0.70, 0.4, 0.45, 0.45, 1.00 for u', F411, g', r', i' and PaJ/Ca II.

at the FAME sensitivity level ($\sim$ 10 mmag at V=15). Clearly, the color-color transformations are highly non-linear and depend significantly upon the composition and pressure of the stellar atmosphere.

Since stars are so different in their spectral/photometric properties, it appears that transformations between photometric systems only makes sense if *identically the same* stars are compared photometrically. Furthermore, accurate relations between photometric systems can only be established for subsets of stars that have similar $log(g)$ and $[Fe/H]$. For example, the largest difference between g'-r' and B-V occurs for g'-r' $\sim$ 0.5 for near-Solar metallicities and gravities. These difference increase towards lower metallicities and lower gravities.

6. Conclusions

The experimentations I have reported on above indicate that:

- a u' filter is mostly useful for metallicity calibration in hot stars ($T_{eff} \gtrsim 10,000$K). It is also of some help for the gravity calibration of G-type stars. The improvements with respect to the NO-u' case are, respectively, $\sim$0.4 dex and 0.1 dex.
- A reasonable substitute for the u' band is the F466 band.
- NO-u' filter sets with either g' or Mg b perform about equally well.
- Lists of standard stars with a range in gravity and metallicity and accurate photometry need be compiled for the external calibration of FAME data.
- Filter sets that *do* include a u' filter should employ the narrower and shifted F411 band rather than the F423 band employed in FTM2001-03.
- Classification results are fairly insensitive to CCD area allocation details.

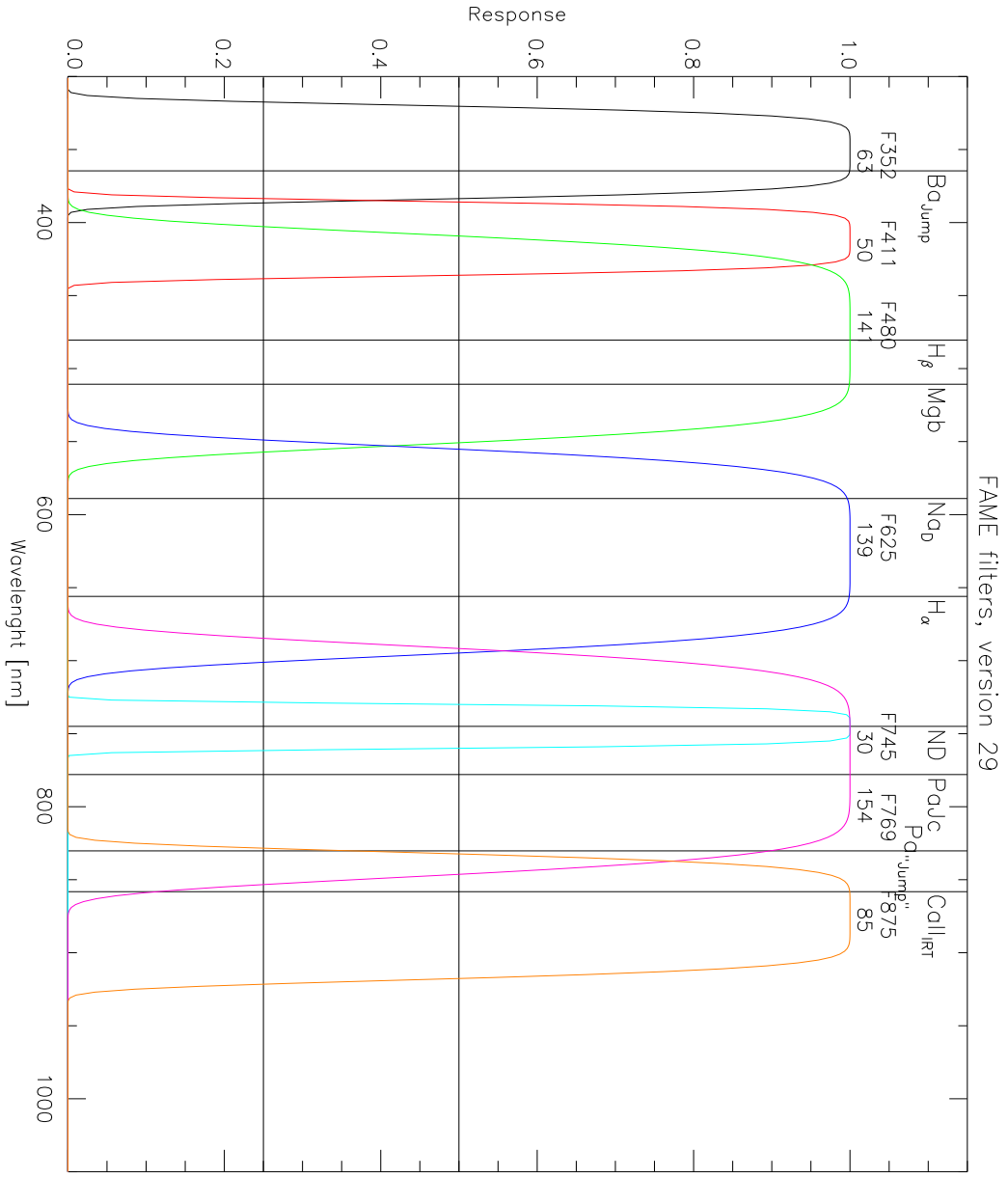

Fig. 1.— The 7-band filter system as presented in table 1. The central wavelengths and widths of the bands (in nm) are indicated above each band. Some astrophysically interesting features are also indicated.

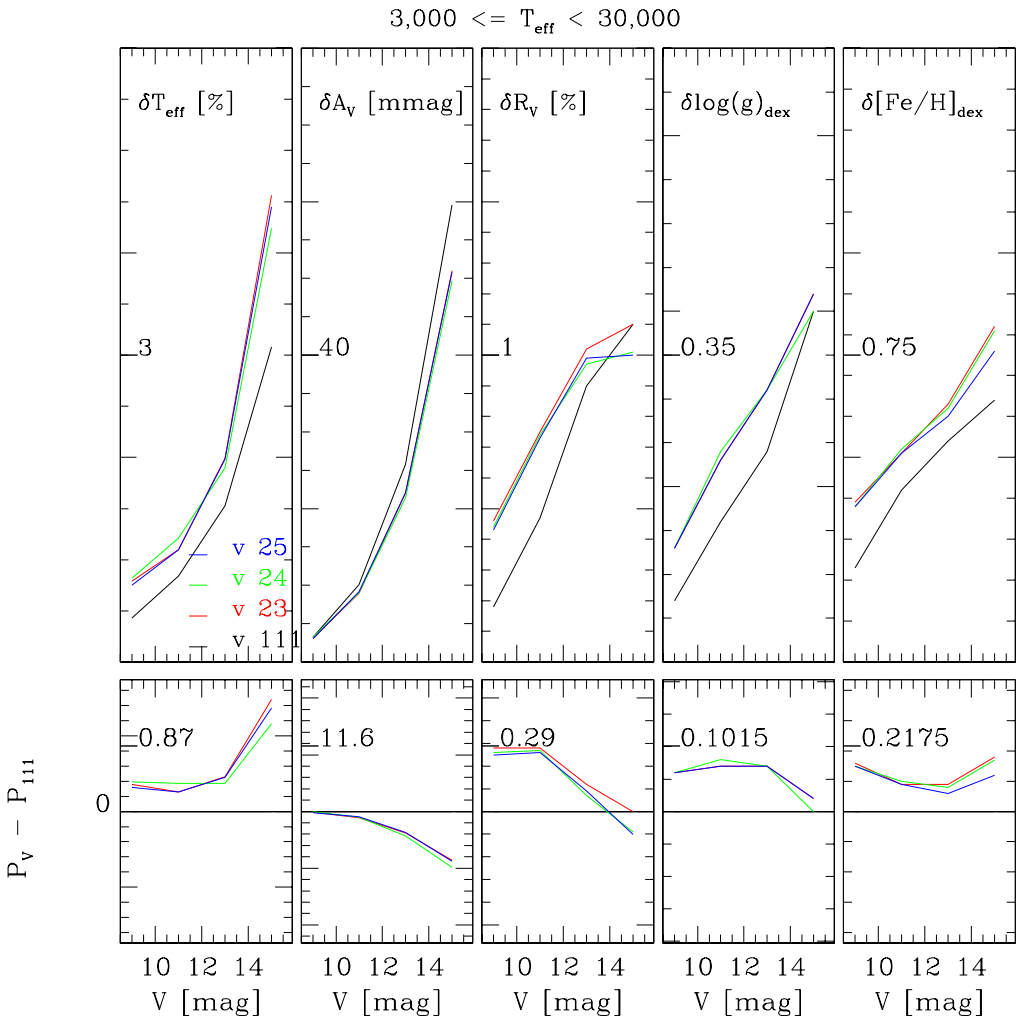

Fig. 2.— F&C classification results for various versions a 6+1 filter system *without* a u' band. In the top panels, I plot the classification errors for T_{eff}, A_V, R_V, $log(g)$ and $[Fe/H]$, from left to right. The units are: %, mmag, %, dex and dex, respectively. In each panel the half-way point of the vertical scale is indicated, whereas all scales start at zero (e.g., T_{eff} is plotted from 0 to 6%). Each incarnation of the filterset is indicated by a different color, and identified in the T_{eff} panel as v #. In the bottom panels, I plot the classification results with respect to version #111.**#111 is the 8-band system as proposed in FTM2001-03 and includes a u' band and employs the TiO-continuum band for bright stars.**; #23 like 111, but no u', and g' replaced by a F466 band; #24 like #111, but no u'; #25 like 111 but no Mg b band; #26 like #23 but with slightly changed bandpasses so as to resemble the blue part of the Strömvil system..

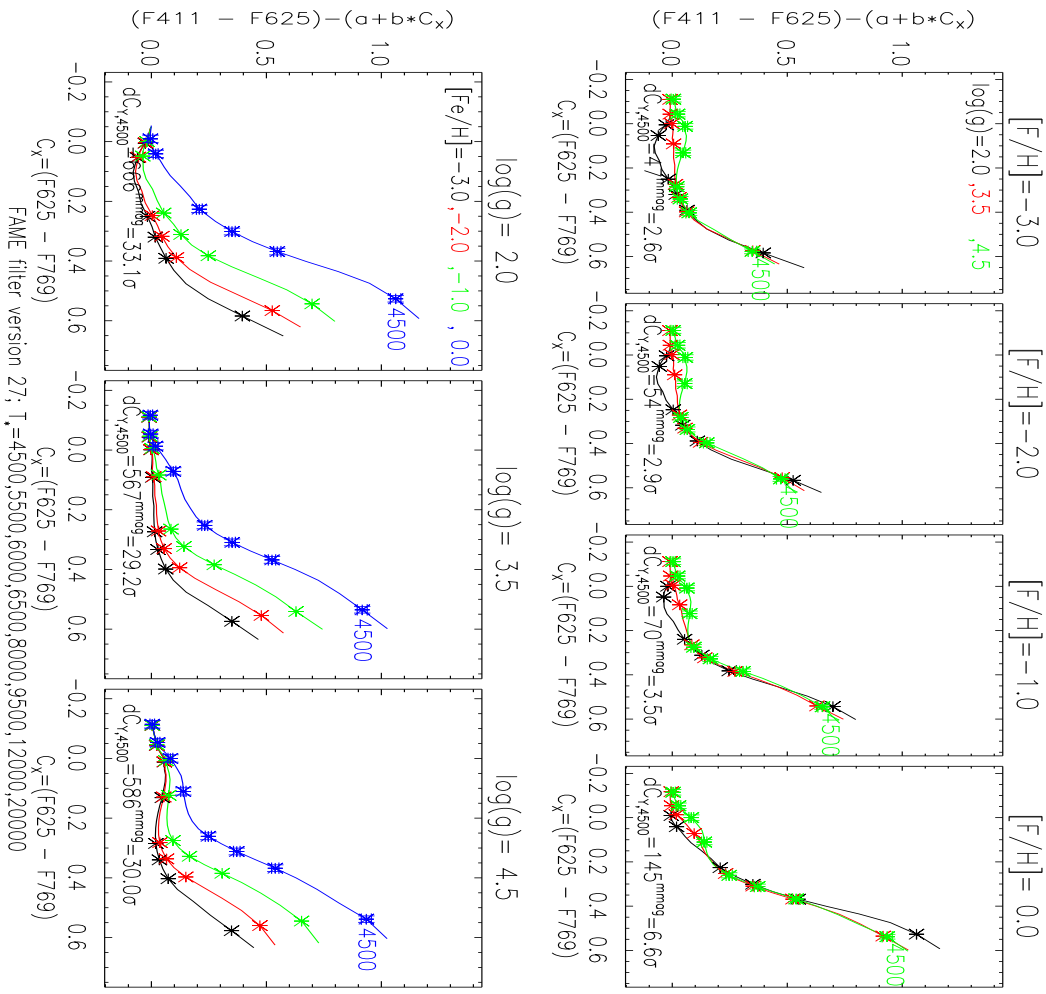

Fig. 3.— A color-color plot for r'-i' (abscissa) and F411-r' (ordinate). The average linear relation has been subtracted. This plot clearly shows the metallicity classification possibilities for F to K stars ($T_{eff} \lesssim 8,000$K). The three **bottom panels** are calculated at fixed surface gravity: 1.5, 3.0, and 4.5 from left to right. The colored curves are for four metallicities: $[Fe/H]$=-3, -2, -1, 0 (black [lower curve], red, green and blue [upper], respectively). Each curve represents a temperature sequence. The asterisks mark the T_{eff} values listed in the sub-title of the figure (the 4,500K value is labeled). The $[Fe/H] = 0$ points include error bars for V=15. These errors are specific to the corresponding stellar atmosphere and FAME's throughput & the allocated CCD-area (tab. 1). In the four **top panels**, each panel has a fixed metallicity: -3,-2,-1,0, from left to right. Each colored line is generated at fixed gravity: $log(g)$=1.5,3.0,4.5 (black, red and green). In this case, the error bars are included for the $log(g)$=4.5 (green) case. In each panel, and for $T_{eff} = 4,500$K, the maximum color difference is indicated, in mmag and units of the rms error in the color (σ). The separation in the ordinate between metal-poor and metal-rich stars is 500-600 mmag (30 σ), so that metallicity for K stars can be determined to approximately 0.1 dex. Note that this color-color plot shows hardly any gravity variation between main-sequence stars and sub giants [$log(g) = 4.5$ & 3.5].

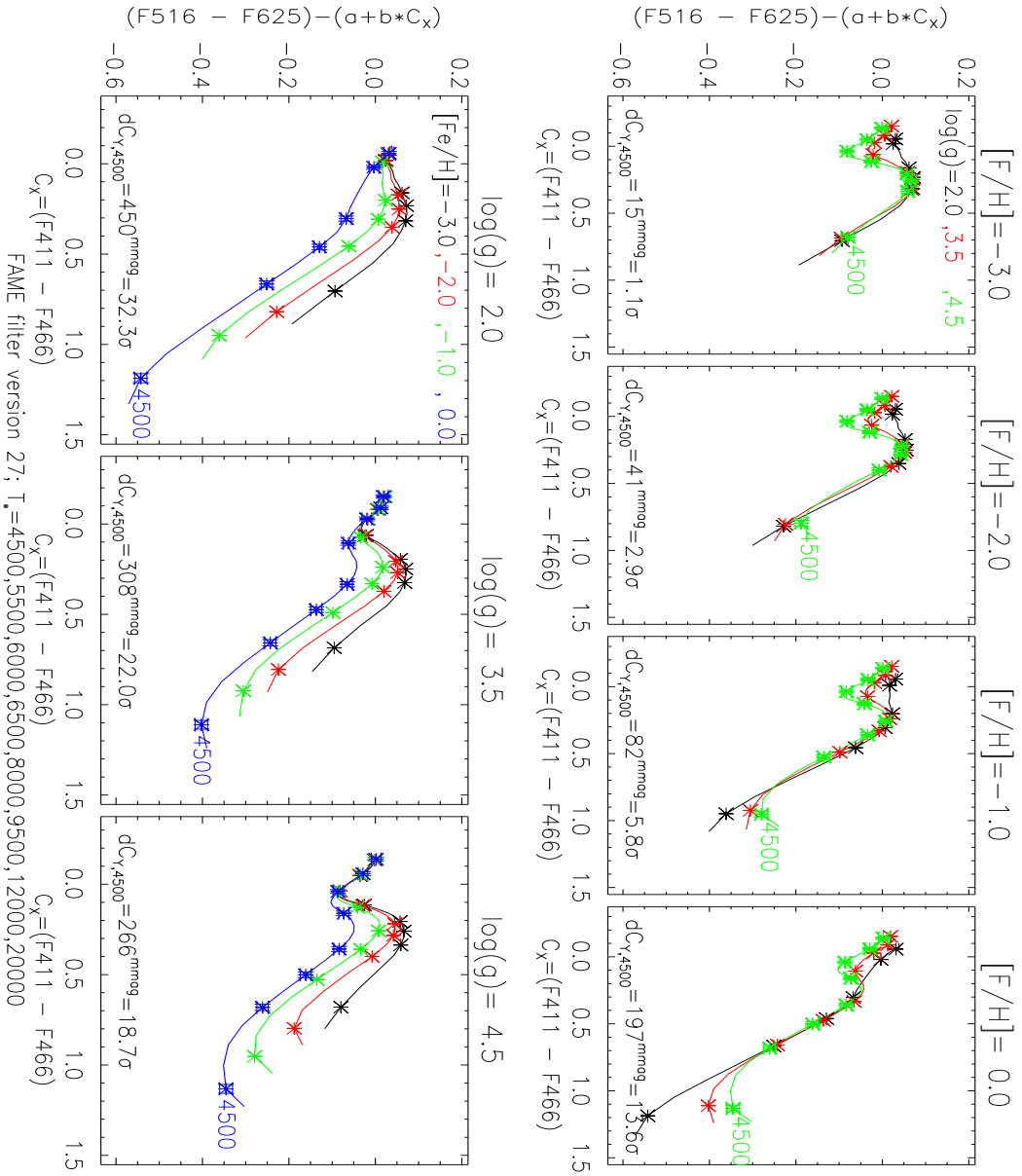

Fig. 4.— Same as figure 3 but F411-F466 versus Mg b-r'. In this case we see that surface gravity discrimination is better (0.2 dex at $T_{eff} = 4,500$K and $[Fe/H] = 0$) than for figure 3. However, for late-type stars at low metallicities, the Mg b line is no longer a good gravity indicator (cf. the Introduction). For A-type stars, this color-color combination is a fair gravity indicator (0.25 dex at $T_{eff} = 9,500$K).

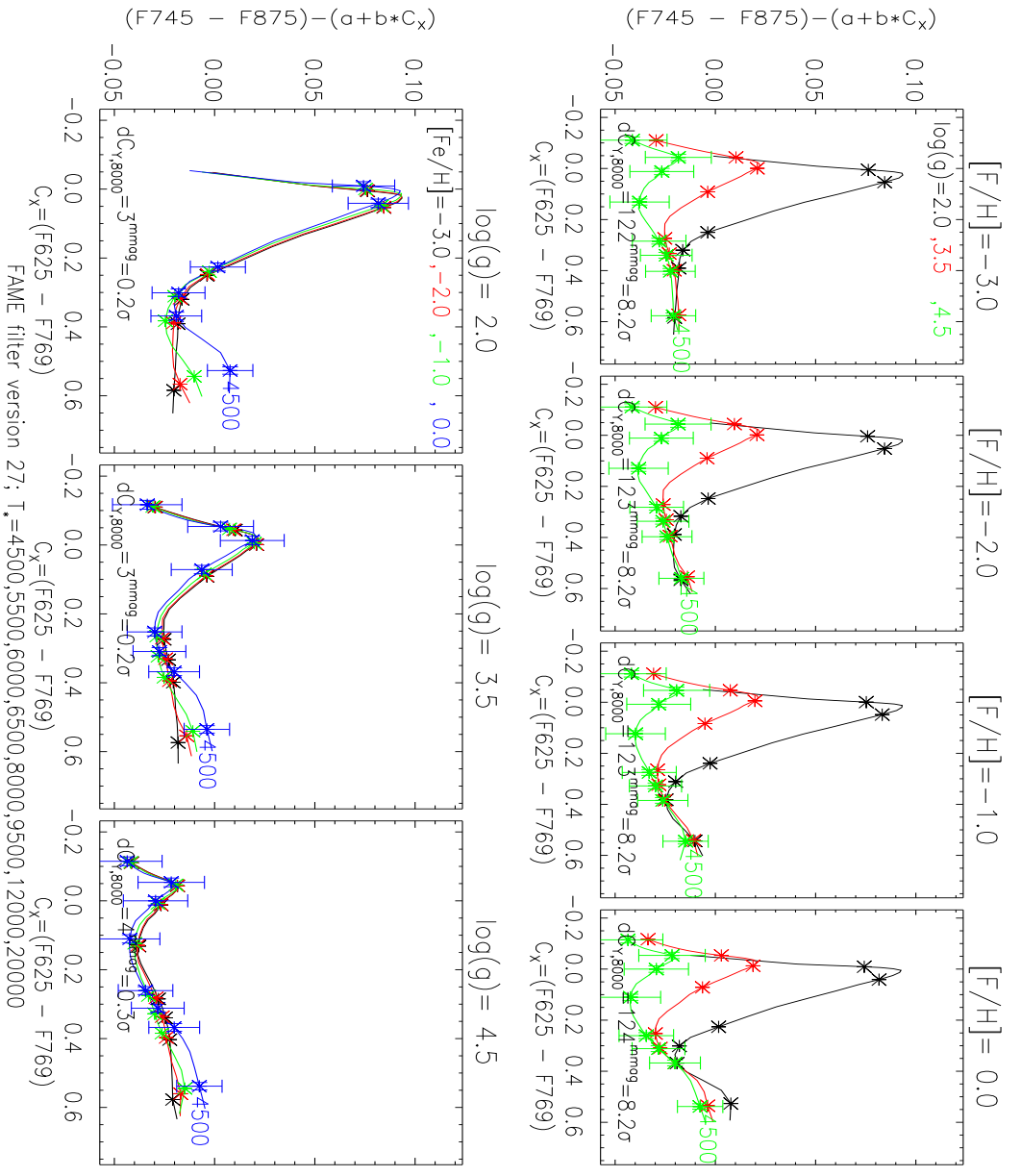

Fig. 5.— Same as figure 3, r'-i' versus TiO_C-PaJ/Ca II. Note that very similar plots are obtained when TiO_C is replaced by either r' or i'. The surface-gravity resolution between 7,000K and 10,000K (the blue part of the instability strip) is about 0.4 dex.

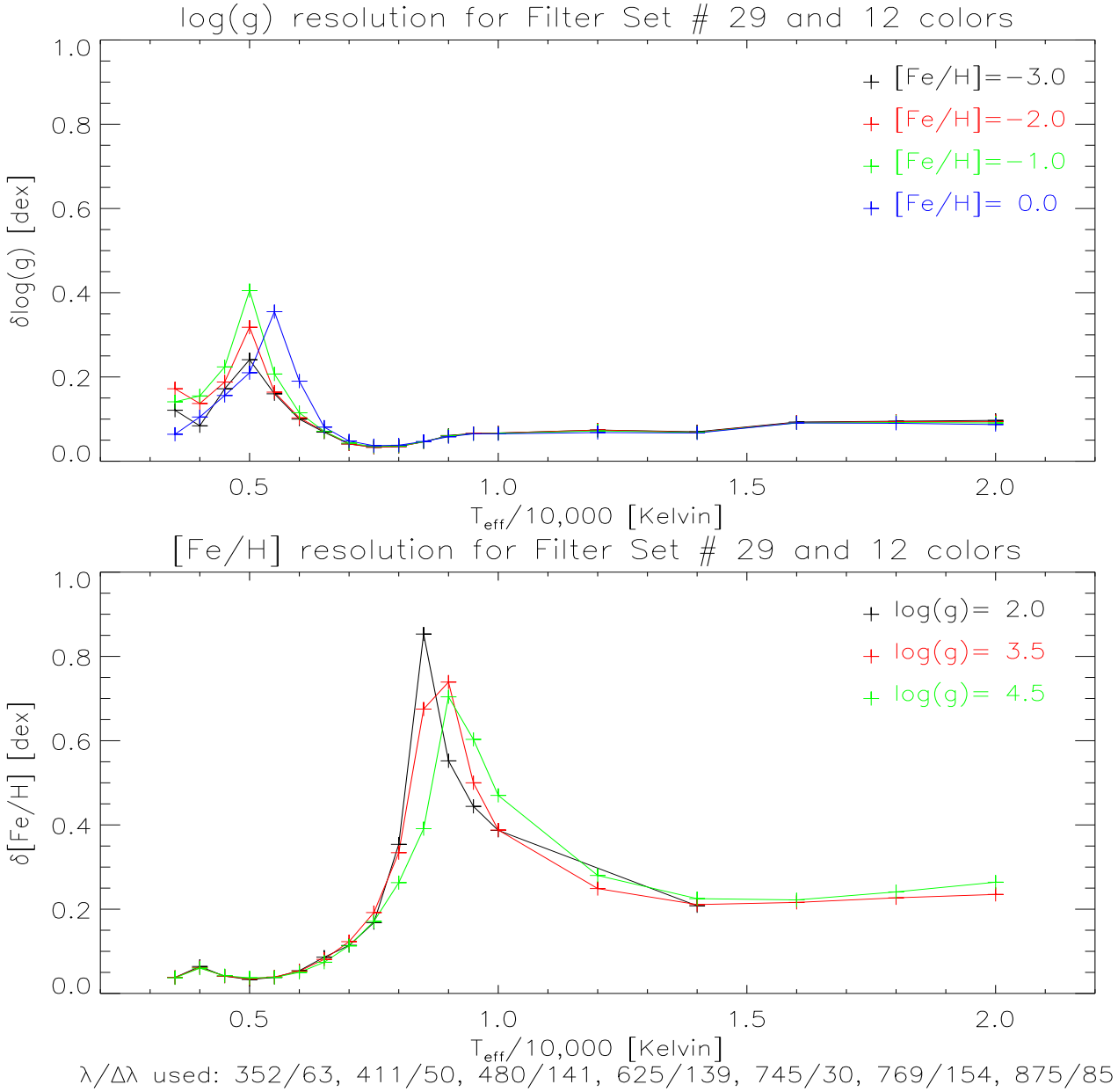

Fig. 6.— The "best possible classification results" derived from equation 1. This filter set contains a u' filter. The central wavelengths and bandwidths of filter set #22 are enumerated below the bottom panel.

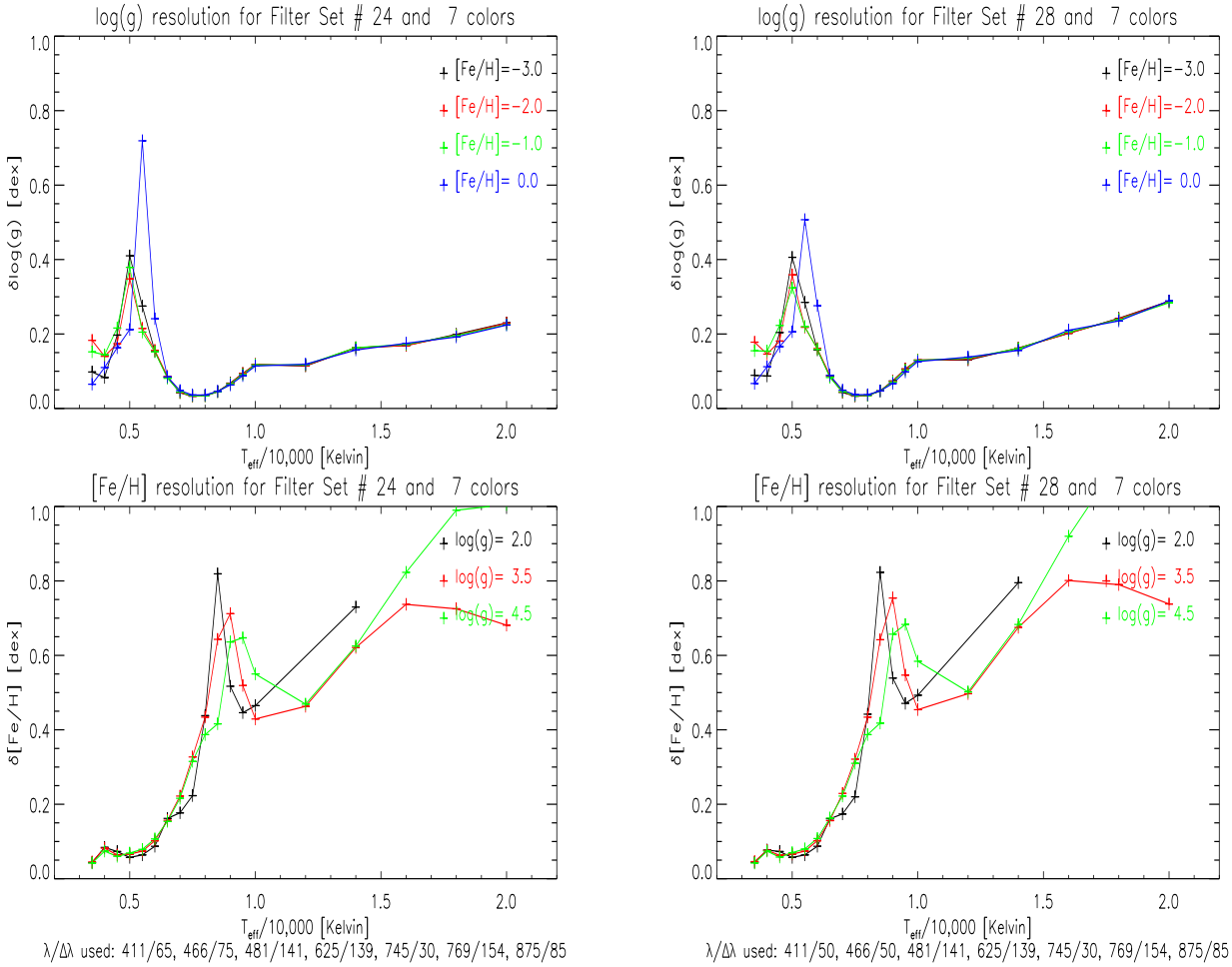

Fig. 7.— The figure caption for both panels is like figure 6. However, the u' band has been replaced by the F466 band. As compared to the YES-u' results of the previous figure, the NO-u' metallicity resolution for O/B stars is strikingly worse. The left- and right-hand panels are for the same filter sets, but the right-hand set has narrower filters, which leads to substantially better classification results.

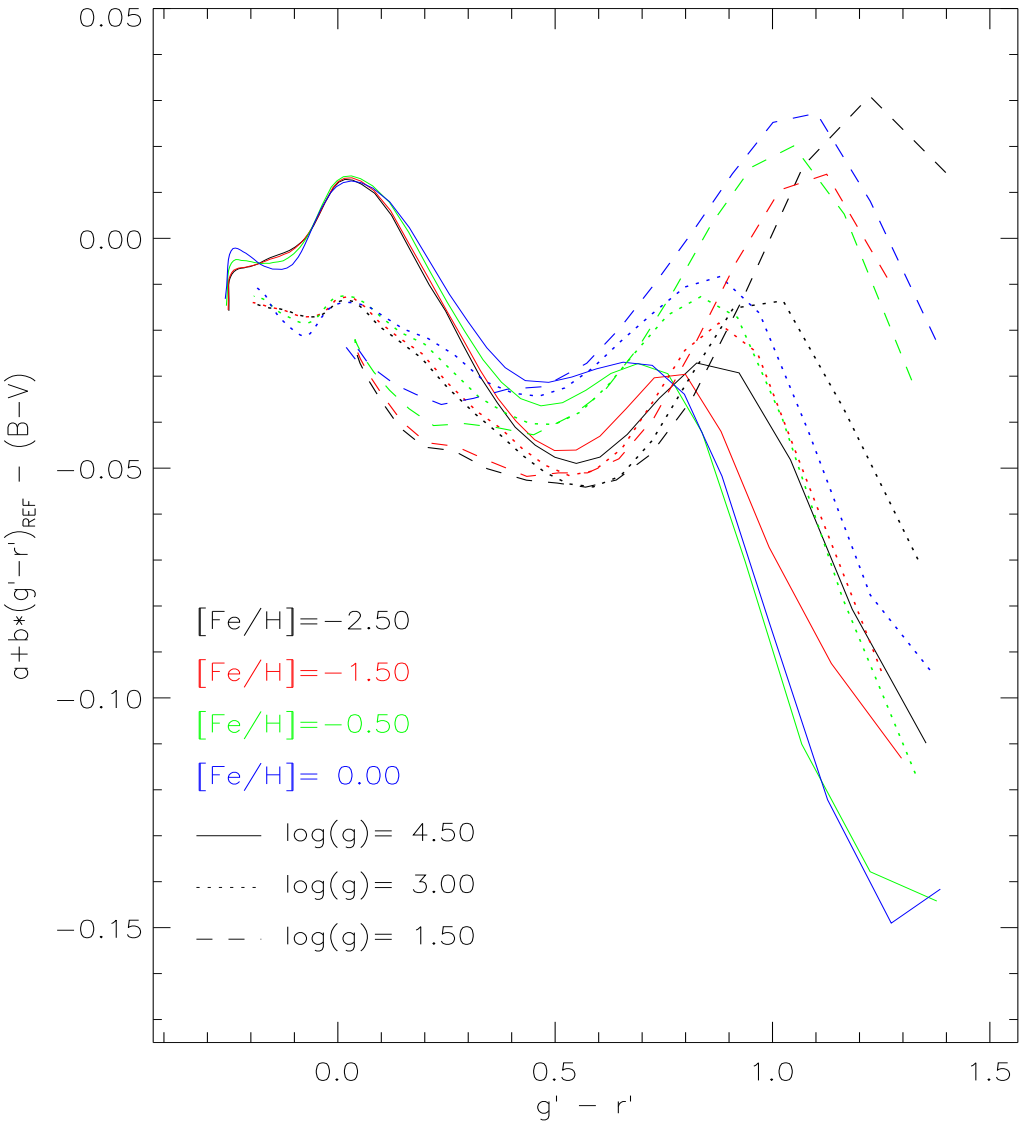

Fig. 8.— In this figure I illustrate the highly non-linear relation between the SDSS (g'-r') color and the Johnson (B-V) color, for various stellar models. On average, these colors are related through an approximately linear relation. I have determined that linear relation for a set of models with Solar metallicity ($[Fe/H = 0.0]$) and main-sequence gravity $[log(g) = 4.5]$. This reference relation has been subtracted from all model color-color plots presented. The following color coding has been used: blue for Solar metallicity models, green for $[Fe/H] = -0.5$, red for $[Fe/H] = -1.5$, and **black** $[Fe/H] = -2.5$. The drawn lines are for "main-sequence" stars, dotted lines for $log(g) = 3$ and dashed lines for $log(g) = 1.5$.